Available online at www.sciencedirect.com
SCIENCE DIRECT®
International Journal of Heat and Mass Transfer 47 (2004) 1657–1671
International Journal of HEAT and MASS TRANSFER
www.elsevier.com/locate/ijhmt

An analysis of black liquor falling film evaporation

Fang C. Chen *, Zhiming Gao

Oak Ridge National Laboratory, P.O. Box 2008, Oak Ridge, TN 37831-6070, USA

Received 17 January 2003; received in revised form 28 October 2003

Abstract

Scaling in conventional black liquor evaporators has presented problems for decades, impeding the improvement of productivity in paper mills. Recent investigations suggest that falling film technology may effectively minimize black liquor fouling and improve productivity in a paper mill. This finding motivates the current work to analyze the transport phenomenon, enrichment and scale fouling of black liquor in a falling film evaporator. In the paper, a mathematical model based on a turbulent two-phase flow with multiple components is presented to investigate the transport processes of black liquor in a falling film evaporator. A phenomenological model of crystallization fouling is used to predict the fouling process. The results show the relationship between heat and mass transfer occurring within a very thin viscous sublayer close to the heat transfer surface, and the influence of soluble solids concentration and thermal boundary condition on the enrichment and scale fouling of black liquor.

1. Introduction

Black liquor, the by-products of the chemical recovery loop in the pulping and paper industry, is a highly viscous alkaline organic mixture that includes water, lignin, cellulose, and inorganic sodium salts [1]. Sodium carbonate (Na_2CO_3) and sodium sulfate (Na_2SO_4) are the major inorganic species in black liquor, and both sodium salts contribute to the formation of encrustations in conventional black liquor evaporators. Sodium carbonate and sodium sulfate form the double salt burkeite ($2Na_2SO_4 \cdot Na_2CO_3$) when they co-crystallize [2,3]. In a modern pulping mill, a multi-effect evaporator system is usually designed to concentrate black liquor from 14–18% up to 68%. However, soluble scale fouling does occur in a conventional black liquor evaporator, which is an obstacle to improving productivity in a pulping mill [3].

Pioneering work by Grace [4] at the Institute of Paper Science and Technology (IPST) in the 1970s showed that soluble scaling in long-tube vertical (LTV) evaporators always occurred if black liquor were concentrated above the solubility limit of Na_2SO_4 and Na_2CO_3. Grace called this concentration the "critical solids" point for soluble scale formation. Süren [5] found that a solids concentration of approximately 48% was the beginning point of scale formation for typical black liquor. Several empirical correlations have been advanced to predict the critical solids point [6,7].

The soluble scale fouling of black liquor is not only a concentration-driven process, but also a heat-sensitive development. These dissolved salts display an abnormal behavior of reduced solubility with increased temperature. The limit of the salts may be exceeded if black liquor is enriched to produce a high concentration of solids. The result will be precipitation both in the bulk solution and on heat transfer surfaces, leading to a heat transfer coefficient drop [8].

The contact time between black liquor and a heated surface is critical to controlling soluble scale fouling. In the pulp and paper industry, the conventional technology used in black liquor evaporators is rising film evaporators, in which the black liquor feed enters the bottom of the steam-heated tubes and flows up inside them. The soluble scale fouling occurs due to the supersaturation of black liquor suspending in the evaporator. In falling film evaporators, however, the black liquor enters at the top; and a thin, fast-flowing film immediately coats the wall as a result of gravity. This

* Corresponding author. Tel.: +865-574-0712; fax: +865-574-9338.
E-mail address: chenfc@ornl.gov (F.C. Chen).

0017-9310/$ - see front matter © 2003 Elsevier Ltd. All rights reserved.
doi:10.1016/j.ijheatmasstransfer.2003.10.034

Nomenclature

a	thermal diffusivity (m^2/s)
c^b	soluble solid concentration (%)
c^w	water component concentration (%)
C_b	soluble solid mass concentration (kg/m^3)
C_D	drag function
c_p	specific heat (kJ/kg K)
C_s	concentration at surface (kg/m^3)
d_l	droplet diameter of liquid phase (m)
D	mass diffusivity (m^2/s)
E_{act}	activation energy (J/mol)
$\vec{F}$	interaction momentum between phases
$\vec{g}$	gravity vector (m/s^2)
h_{fg}	heat of evaporation (kJ/kg)
K_{ji} or K_{ij}	interface momentum exchange coefficient between jth phase and ith phase ($kg/s\,m^3$)
L	length of falling film (m)
m	mass (kg)
$\dot{m}_{ji}$	mass transfer from jth phase to ith phase ($kg/s\,m^3$)
$\dot{m}_{ij}$	mass transfer from ith phase to jth phase ($kg/s\,m^3$)
P	pressure (Pa)
Pr_t	turbulent Prandtl number
R	perfect gas constant (8.314 kJ/kmol K)
Re	Reynolds number, $Re = 4\Gamma/\mu$
R_f	fouling resistance (m^2K/kw)
r_{lv}, r_{vl}	evaporation and condensation coefficient
Sc_t	turbulent Schmidt number
T	temperature (K)
T_s	fluid-deposit interface temperature (K)
u	velocity at x direction (m/s)
$\mathbf{U}$	velocity vector (m/s)
v	velocity at y direction (m/s)
W	$Na_2CO_3 + Na_2SO_4$ wt% on total black liquor solid
x	stream-wise coordinate
$\mathbf{X}$	position vector
y	transverse coordinate
W	channel width if falling film evaporator (m)
Z	effective sodium (%) on total black liquor solids

Greek symbols

α	volume fraction
μ	dynamic viscosity ($N\,s/m^2$)
ρ	density (kg/m^3)
ρ_{bl}	black liquor density (kg/m^3)
ρ_d	deposit density (kg/m^3)
Γ	mass flow rate per unit film width for a planar film (kg/m s)
k	turbulent kinetic energy (m^2/s^2)
ε	turbulent dissipation rate (m^2/s^3)
θ	time (s)
λ_d	deposit thermal conductivity (w/m K)

Subscripts

0	initial condition
c	condensation
e	evaporation
eff	effective transport coefficient
i or j	ith phase or jth phase
ij or ji	interface between ith phase or jth phase
in	inlet
l	liquid
lv or vl	transfer between liquid and vapor phases
m	mixing
sat	saturated
t	turbulent
s	solid
v	vapor
w	wall

process leads to a short contact time, a high heat transfer coefficient, and a low pressure drop. Recent investigations have found that falling film technology could minimize the fouling of black liquor if it were employed in both evaporators and high-solids concentrators [1]. Falling film evaporators become an attractive alternative to conventional black liquor evaporators in many pulping and paper mills.

Falling film technology has been found in a wide variety of engineering application, although it is still a new innovation in pulping and paper industry [9]. Since Nusselt [10] determined the theoretical stream-wise velocity profile for a liquid film at the free interface in 1916, a significant amount of research on falling film hydrodynamics—both experimental work and theoretical analyses—has been conducted over the last few decades [11]. Most of this research was carried out on laminar film and waviness of the gas–liquid interface [12,13]. Solutions of water and propylene glycol were usually used to form thin films in these studies.

Research on transport phenomena in falling films was reviewed by Seban [14] and by Killion and Garimella [15]. Seban and his coworkers [16,17] theoretically investigated evaporation from a liquid water film into a pure water vapor. Their studies focused on the transport process in the liquid film. A similar analysis was carried out by Yüksel and Schlünder [18]. Several of the earlier studies focused on heat and mass transfer in the gas flow, in which the very thin liquid film was assumed to

be replaced by appropriate boundary conditions. These kind of studies were carried out over flat plates or inside a circular pipe [19,20]. The transport process in both gas flow and liquid film has been analyzed by Shembharkar and Pai [21], Baumann and Thiele [22], Yan [23], and Tsay and Lin [24]. Although they considered turbulent gas flow, liquid film was still assumed as laminar. The major difference among them was the definition of liquid film temperature profile. The first two assumed the temperature profile across the film was linear, and the later two considered the profile as fully developed laminar.

The literature reviewed did not accurately reflect the coupled relationship of transport process in a black liquor falling film evaporator. Black liquor falling film evaporation is a two-phase flow because the evaporation process occurs along a near-vertical heat transfer surface. Heat and mass transfer within black liquor falling film takes place between the liquid and vapor phases. The driving forces of the transport phenomena vary with the local temperature, soluble solids concentration gradient, and equilibrium condition at the interface between liquid and vapor. When the black liquor solids concentration is beyond its solubility limit, precipitation will occur in the bulk solution, leading to deposition and fouling on the heat transfer surface [6]. Hence, understanding the transport processes and soluble solids concentration profile of black liquor is important for utilizing black liquor falling film evaporators in a modern paper mill. The thermal properties of black liquor also affect the transport processes. The Prandtl number of black liquor is ten times higher than that of water. For a film of a given Reynolds number, a typical film thickness of black liquor could be more than an order of magnitude greater than that of water. Thus the performance of a falling film of black liquor is significantly different from that of a film of water or other low-viscosity fluids.

Considered little is known about the performance of black liquor falling film evaporators, the present effort will be useful in improving productivity for the pulp and paper industry. The current work is to numerically simulate the transport, enrichment, and scaling of black liquor in a falling film evaporator, in conjunction with the corresponding experimental work carried out at Georgia Tech [1] and IPST [32]. A set of mathematical formulae based on volume fraction is presented to describe a turbulent two-phase flow with multi-species. A two-dimensional computational fluid dynamics code is employed to investigate the transport processes of a black liquor falling film evaporator, coupled with a modified empirical model for analyzing the scale fouling of black liquor. The simulation includes the fluid flow and heat transfer, and the enrichment and scaling of black liquor in a falling film evaporator.

2. Mathematical model

2.1. General

In a black liquor falling film evaporator, black liquor feed enters at the top of the evaporator, flows downward along the steam-heated surface in the form of a film, and leaves from the bottom. Vapor separated from the liquid is carried aloft and exits at the top. Fig. 1 is a schematic of the falling film evaporator considered in the study. The heated surface is a vertical plate subjected to a uniform high temperature. As mentioned earlier, black liquor is a multi-component fluid. The evaporation of water species in black liquor will result in black liquor enrichment. Therefore, black liquor falling film includes vaporized water and enriched black liquor. The vaporization process leads the film developed into a turbulent flow.

As shown in the schematic of the falling film evaporator, the basic assumptions made include these: (1) black liquor consists of water and soluble black solids; (2) a black liquor falling film is considered as a two-phase flow, including vapor and enriched black liquor; (3) precipitates are assumed not to affect the hydrodynamic characteristics of the vapor–liquid flow; (4) the turbulent transport is described through adding an eddy transport coefficient to the molecular ones, and effective transport coefficients are given by $\mu_{\text{eff}} = \mu + \mu_{\text{t}}$, $a_{\text{eff}} = a + a_{\text{t}}$, $D_{\text{eff}} = D + D_{\text{t}}$; and (5) momentum and mass exchanges are considered between phases.

2.2. Governing equations

Governing equations of the fluid flow in the falling film evaporator are based on a two-phase model. The fluid flow is considered to consist of thin falling film and

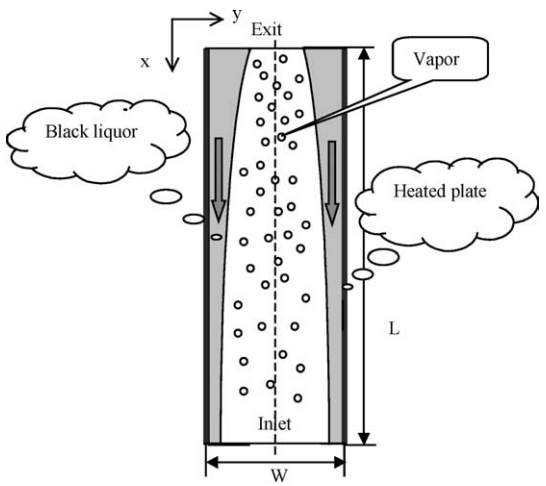

Fig. 1. Schematic of falling film evaporator.

uprising vapor. The thin falling film is a two-phase flow along the heated wall, and the uprising vapor is a single-phase flow in the center. The flow is considered in two dimensions. The position vector, $\mathbf{X}$, expressed in Cartesian coordinates, is given as $\mathbf{X} = xi + yj$; the vapor and liquid fluid velocity vectors, $\mathbf{U}_i$, are given by $\mathbf{U}_i = u_i i + v_i j$.

The concept of volume fraction is employed to analyze the multiphase flow, as well as the mass and momentum transfer between vapor and liquid phases. Volume fraction represents the volume occupied by each phase. The conservation equation of volume fraction is described as $\sum \alpha_i = 1$. Based on the concept of volume fraction, the laws of conservation of mass, momentum, energy, and species are satisfied by each phase individually.

The conservation of mass, which governs the ith phase in the multiphase flow, is given by

$$\mathbf{U}_i \cdot \nabla \alpha_i = \frac{\dot{m}_{ji}}{\rho_i}, \tag{1}$$

where $\dot{m}_{ji} = -\dot{m}_{ij}$.

The momentum conservation for the ith phase in the multiphase flow is described as

$$\nabla \cdot (\alpha_i \mathbf{U}_i \mathbf{U}_i) = -\frac{1}{\rho_i}\nabla P + \frac{1}{\rho_i}\nabla \cdot S_i + \alpha_i \vec{g} + \frac{\vec{F}_{ji}}{\rho_i}, \tag{2}$$

where $\vec{g}$ is only in the x-direction, and the stress tensors $\nabla \cdot S_i$ are given by

$$\nabla \cdot S_i = \nabla \cdot (\alpha_i \mu_{i,\mathrm{eff}} \nabla \mathbf{U}_i). \tag{3}$$

The last term in Eq. (2) is the interaction term that includes momentum exchange and mass exchange at the interface of phases, as described by

$$\vec{F}_{ji} = -\vec{F}_{ij} = K_{ji}(\mathbf{U}_j - \mathbf{U}_i) + \dot{m}_{ji}\mathbf{U}_{ji}. \tag{4}$$

Note: In Equation (4), if mass transfer occurs from the jth phase to the ith phase ($\dot{m}_{ji} > 0$), $\mathbf{U}_{ji} = \mathbf{U}_j$; otherwise, $\mathbf{U}_{ji} = \mathbf{U}_i$; so it is given by

$$\dot{m}_{ji}\mathbf{U}_{ji} = \max\lfloor 0, \dot{m}_{ji}\rfloor \mathbf{U}_j - \max\lfloor 0, -\dot{m}_{ji}\rfloor \mathbf{U}_i. \tag{5}$$

To predict the heat and mass transfer within the multiphase flow, an energy equation is presented for the ith phase as follows:

$$\nabla \cdot (\alpha_i \mathbf{U}_i T_i) = \nabla \cdot (a_{i,\mathrm{eff}} \nabla T_i) + \frac{\dot{m}_{ji} h_{\mathrm{fg}}}{\rho_i c_{pi}}. \tag{6}$$

Since black liquor is considered to include a water component and soluble black liquor solids, the conservation equation of the mass fraction of the water component and soluble black solids can be described as unity: $c_i^{\mathrm{b}} + c_i^{\mathrm{w}} = 1$. An additional conservation equation is required for predicting the mass fraction of the water or soluble black liquid solids in the liquid phase. The equation is given as

$$\nabla \cdot (\alpha_i \mathbf{U}_i c_i^{\mathrm{b}}) = \nabla \cdot (\alpha_i D_{i,\mathrm{eff}} \nabla c_i^{\mathrm{b}}) + \dot{c}_i^{\mathrm{b}}, \tag{7}$$

where $\dot{c}_i^{\mathrm{b}}$ is caused by the water mass exchange between liquid and vapor phases, and $\dot{c}_i^{\mathrm{b}} = -\dot{c}_i^{\mathrm{w}}$.

2.3. Momentum and mass transfer at the interface of phases

As shown in Eq. (4), the momentum exchange at the interface of the vapor and liquid phases is based on the exchange coefficient, K_{ph}. The current falling film is a vapor–liquid flow. The exchange coefficient for this type is described as follows:

$$K_{ji} = \frac{3}{4} C_{\mathrm{D}} \frac{\alpha_j \rho_i |\mathbf{U}_j - \mathbf{U}_i|}{d_{\mathrm{l}}}, \tag{8}$$

where C_{D} is a drag function based on the flow situation. In the current turbulent flow, C_{D} is considered as 0.44. $|\mathbf{U}_j - \mathbf{U}_i|$ is the relative phase velocity between the ith and jth phases.

A simple phenomenological model for a vapor–liquid flow is used to determine the mass transfer between phases, which is described as follows:

$$\text{If } T_{\mathrm{l}} \geqslant T_{\mathrm{sat}}, \quad \dot{m}_{\mathrm{e}} = r_{\mathrm{lv}} \alpha_{\mathrm{l}} \rho_{\mathrm{l}} (T_{\mathrm{l}} - T_{\mathrm{sat}})/T_{\mathrm{sat}}, \tag{9a}$$

$$\text{If } T_{\mathrm{l}} \prec T_{\mathrm{sat}}, \quad \dot{m}_{\mathrm{e}} = 0, \tag{9b}$$

$$\text{If } T_{\mathrm{v}} \leqslant T_{\mathrm{sat}}, \quad \dot{m}_{\mathrm{c}} = r_{\mathrm{vl}} \alpha_{\mathrm{v}} \rho_{\mathrm{v}} (T_{\mathrm{sat}} - T_{\mathrm{v}})/T_{\mathrm{sat}}, \tag{9c}$$

$$\text{If } T_{\mathrm{v}} \succ T_{\mathrm{sat}}, \quad \dot{m}_{\mathrm{c}} = 0. \tag{9d}$$

Therefore,

$$\dot{m}_{\mathrm{lv}} = -\dot{m}_{\mathrm{vl}} = \dot{m}_{\mathrm{e}} - \dot{m}_{\mathrm{c}}. \tag{10}$$

Only the mass exchange caused by evaporation and condensation is considered here because mass transfer caused by other reasons is relatively slight.

2.4. Eddy transport coefficients

Turbulent transport is considered through adding eddy transport coefficients into molecular coefficients; the results are called effective transport coefficients, such as $\mu_{\mathrm{eff}} = \mu + \mu_{\mathrm{t}}$, $a_{\mathrm{eff}} = a + a_{\mathrm{t}}$, $D_{\mathrm{eff}} = D + D_{\mathrm{t}}$.

The thermal eddy diffusivity a_{t} is caused by the turbulent transport, which is calculated from the eddy viscosity μ_{t} by using a further equation involving the turbulent Prandltl number Pr_{t}.

$$a_{\mathrm{t}} = \frac{\mu_{\mathrm{t}}}{\rho Pr_{\mathrm{t}}}. \tag{11}$$

Although some authors gave a transversal distribution function for the turbulent Prandtl number, the majority of the authors considered Pr_{t} as a constant

value over the film [19]. In the current study, Pr_t is considered as a constant value.

The mass eddy diffusivity is calculated from the eddy viscosity, μ_t, by using an equation involving the turbulent Schmidt number Sc_t

$$D_t = \frac{\mu_t}{\rho Sc_t}, \tag{12}$$

where the turbulent Schmidt Sc_t is assumed to be equal to the turbulent Prandltl number Pr_t.

The eddy viscosity is related to k and ε by the expression

$$\mu_t = \rho C_\mu \frac{k^2}{\varepsilon}, \tag{13}$$

where the coefficient C_μ is an empirical constant that has the empirically derived value $C_\mu = 0.0845$.

The turbulent kinetic energy k and dissipation rate ε in Eq. (13) are determined by the RNG-based k–ε turbulent model. The log-law equation is employed in the current turbulent model to relate the wall shear stress to the fluid velocity at a short distance away from the wall.

2.5. Boundary conditions

In the study, a no-slip wall is considered. The governing Eqs. (1)–(6) are subjected to the boundary conditions. Thus the boundary conditions at the wall followed (refer to Fig. 1) $u_v = u_l = v_v = v_l = 0$ and $T_v = T_l = T_w$ at $y = 0$.

At the interface between vapor and liquid, heat and mass transport are coupled by the governing equations; i.e., Eqs. (1), (2) and (6) are employed to predict the velocity, temperature, and species concentration in the falling film evaporator.

To save computer time, a symmetric mesh is adapted. Thus all gradients at symmetric line (or $y = W/2$, W, the channel width) are considered to be zero; thus $\frac{\partial u_v}{\partial y} = \frac{\partial u_l}{\partial y} = \frac{\partial v_v}{\partial y} = \frac{\partial v_l}{\partial y} = 0$, $\frac{\partial T_v}{\partial y} = \frac{\partial T_l}{\partial y} = 0$, and $\frac{\partial \alpha_v}{\partial y} = \frac{\partial \alpha_l}{\partial y} = 0$ at $y = W/2$.

The initial condition includes the temperature and velocity field. The temperature is considered to be constant, and the velocity profile is assumed to be a static field. Vapor is filled within the initial flow field. The initial value for the profile of velocity, temperature, and concentration are given as $u_v = u_l = v_v = v_l = 0$, $T_v = T_l = T_0$, and $\alpha_v = 1$.

Meanwhile, the inlet conditions are considered to be a uniform profile of velocity, temperature, and concentration. However, falling film is a two-phase flow along the vertical heated surface. The variables, such as temperature and velocity, need a function to express the mixing characteristic in the two-phase flow. Therefore, the following mixing variables are presented as bulk variables of density, temperature, and velocity vector, which are used in analyzing the flow characteristics of two-phase flow.

$$\rho_m = \sum \alpha_i \rho_i, \quad c_{pm} = \sum \alpha_i c_{pi},$$
$$T_m = \frac{\sum \alpha_i \rho_i c_{pi} T_i}{\rho_m c_{pm}}, \quad \text{and} \quad \mathbf{U}_m = \frac{\sum \alpha_i \rho_i \mathbf{U}_i}{\rho_m}. \tag{14}$$

Note that in all the above formulations, the transport properties of black liquor are calculated from Ramamurthy et al. [25] and Zaman and Fricke [8]. The transport properties of vapor come from Incropera and DeWitt [26].

3. Numerical method solution and model validation

On the basis of using the finite-difference method derived by integrating over the meshed control volume, the governing equations for the two-phase flow model are solved through incorporating the SIMPLE algorithm of Patankar and Spalding [27]. Since the governing equations are involved in non-linearity and the coupling of relative variables, iterative numerical procedures are conducted until the convergence is reached. The solution is considered to converge if the sum of the normalized residuals has fallen below a specified level δ, i.e.,

$$\sum |R_n| / R_{n,\mathrm{ref}} \leqslant \delta, \tag{15}$$

where R_n is the local residual of the n equation and $R_{n,\mathrm{ref}}$ ref is the reference quantity. In the current study, the convergence is assumed to be reached when δ is less than 0.001.

To validate the model, two pure liquid falling film flow conditions are considered here: one is the low-Reynolds laminar flow, and the other is high-Reynolds turbulent flow. The results are illustrated in Fig. 2. In Fig. 2(a), the triangle series is the current turbulent simulation; the diamond series is the Nusselt [10] results; the solid and white square series are Adomeit and Renz [13] and Karimi and Kawaji [11], respectively. The Reynolds number of the solid series is 800, and the number of the other series is 2338. Fig. 2(b) illustrates the laminar comparison of the current prediction with experimental data at a low Reynolds number (<50). The triangle series is the current simulation; the solid and white square diamond series are the Nusselt [10] results; the white square series is Portalski [28]; and the solid square series is Wilkes and Nedderman [29]. The results show a fair match with experimental data whether the Reynolds number is low or high. Therefore, the model can predict the performance characteristics of a falling film evaporator with reasonable accuracy.

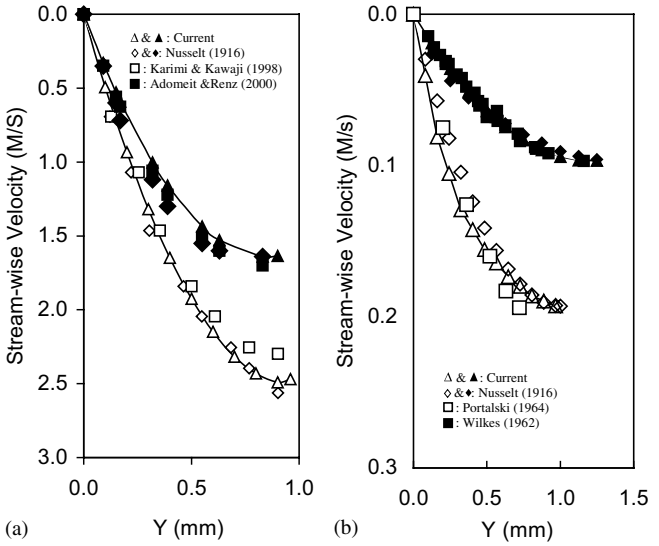

Fig. 2. The comparison of predicted with experimental data; in (a) the Reynolds number of the solid series is 800 and that of the space series is 2338; in (b) the Reynolds number is <50.

4. Numerical analysis and discussion

The geometric scales of falling film evaporators have been determined through laboratory experiments done by Smith and Hsieh [1]. To simulate the transport processes of black liquor falling film, two cases were carried out to reflect both experimental and industrial scales. A 1.8 m-long falling film [1] was employed to investigate the fundamental process of the application of black liquor in a falling film evaporator. Based on the simulation of the 1.8-m-long falling film, a 10 m-long falling film, the scale of an industrial black liquor falling film evaporator, was analyzed. The details are listed in Table 1. All geometries are considered here in two dimensions, and the width of the plate is assumed to be infinite.

Since the soluble black liquor solids composition is affected by the molecular weight distribution of the lignin, the transport properties of black liquor vary with the degree of delignification of wood species. In the current work, only typical black liquor is considered. The composition of soluble solids includes 20% sodium, 9% sodium carbonate, and 2.3% sodium sulfate. The ratios of Na_2CO_3/Na_2SO_4 and organic/inorganic material are assumed as 80:20 and 60:40, respectively. According to the critical solids point model [6], the current critical solids point is around 49%. In the current study, fluid properties are based on the temperature and black liquor solids concentration.

Table 1
Geometric scales of falling film evaporators and the boundary conditions of black liquor

Length of plate (m)	1.8 and 10
Half-width of channel (m)	0.05
Inlet temperature of liquid film (K)	348, 368, and 388
Inlet temperature of vapor stream (K)	348, 368, and 388
Wall temperature (K)	358, 378, and 398
Inlet velocity of liquid phase (m/s)	0.2
Inlet velocity of vapor stream (m/s)	0.3
Inlet falling film thickness (m)	0.01
Inlet solid concentration (%)	35, 40, and 45

4.1. Tranport of black liquor in a 1.8-m falling film evaporator

Since the fluid flow in a falling film evaporator is a two-phase flow, the two-phase film thickness is defined by the distance from the heated surface to the location where the volume fraction of the liquid phase is not less than 1%. All falling film thicknesses in the study follow this definition.

The numerical analysis results of a typical two-phase flow in a 1.8-m-long falling film evaporator are plotted in Fig. 3. In the case, black liquor solids concentration is 40%; inlet black liquor temperature, inlet vapor temperature, and wall temperature are 368, 368, and 378, respectively. As shown in Fig. 3(a), the volume fraction of the liquid phase decreases gradually while the falling film falls down along the heated surface. A liquid falling film is developed into a vapor–liquid flow. In the velocity profile view in Fig. 3(b), the two-phase film seems to move down together. The phenomenon is caused by the density difference in liquid and vapor. For

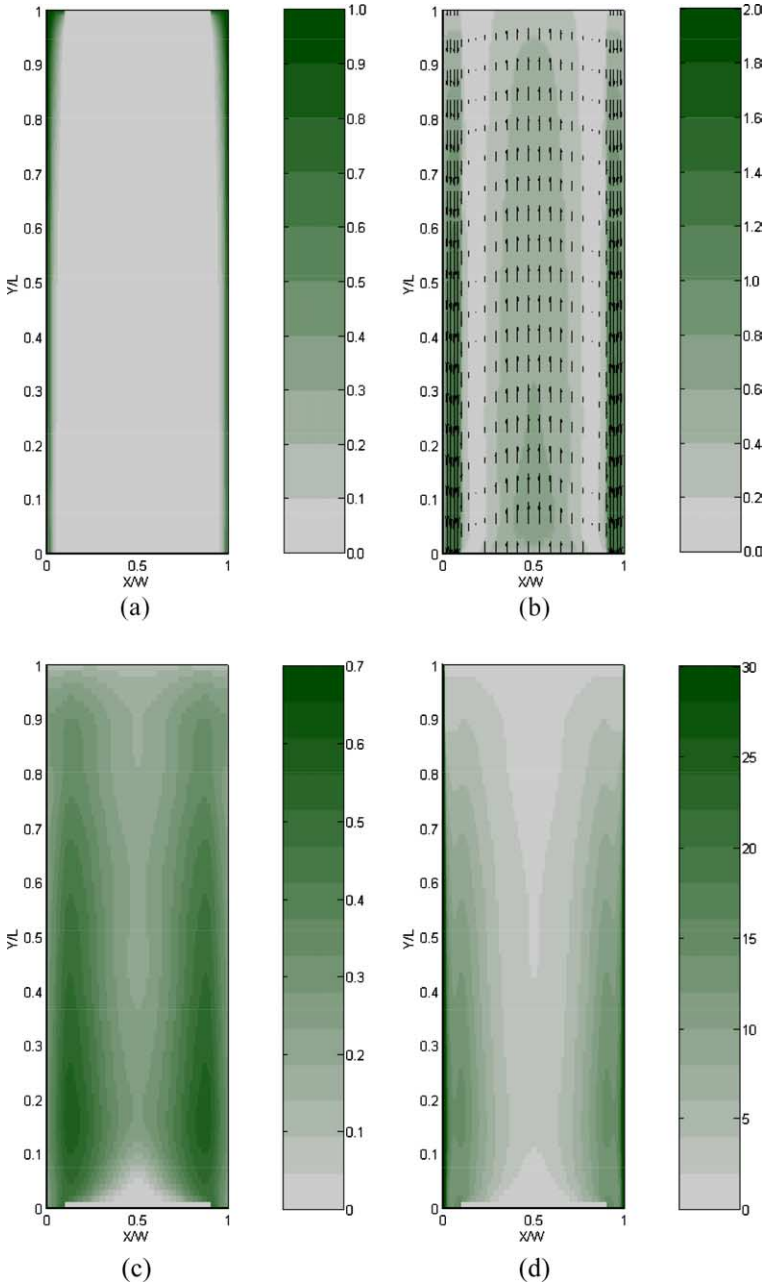

Fig. 3. The prediction of a typical two-phase flow for a 1.8-m-long falling film: (a) volume fraction of liquid phase; (b) velocity profile; (c) turbulent kinetic energy profile; (d) turbulent dissipation profile. The Reynolds and Prandtl number are 2650 and 19.6, respectively.

a control zone with a certain velocity, a small volume fraction of liquid still possesses a higher momentum than vapor because the density of liquid is three orders of magnitude higher than that of vapor. As a consequence, liquid and vapor move together. Fig. 3(c) and (d) illustrate the turbulence and diffusion profile in the falling film evaporator.

Fig. 4 shows the profiles of velocity, temperature, and black solids concentration in a 1.8-m-long thin falling film. In Fig. 4(a), the velocity of the liquid film accelerates under the force of gravity while the falling film periphery contracts to a section smaller than the inlet film thickness because of fluid inertia. This section is known as the ''vena contracta.'' After the vena contracta,

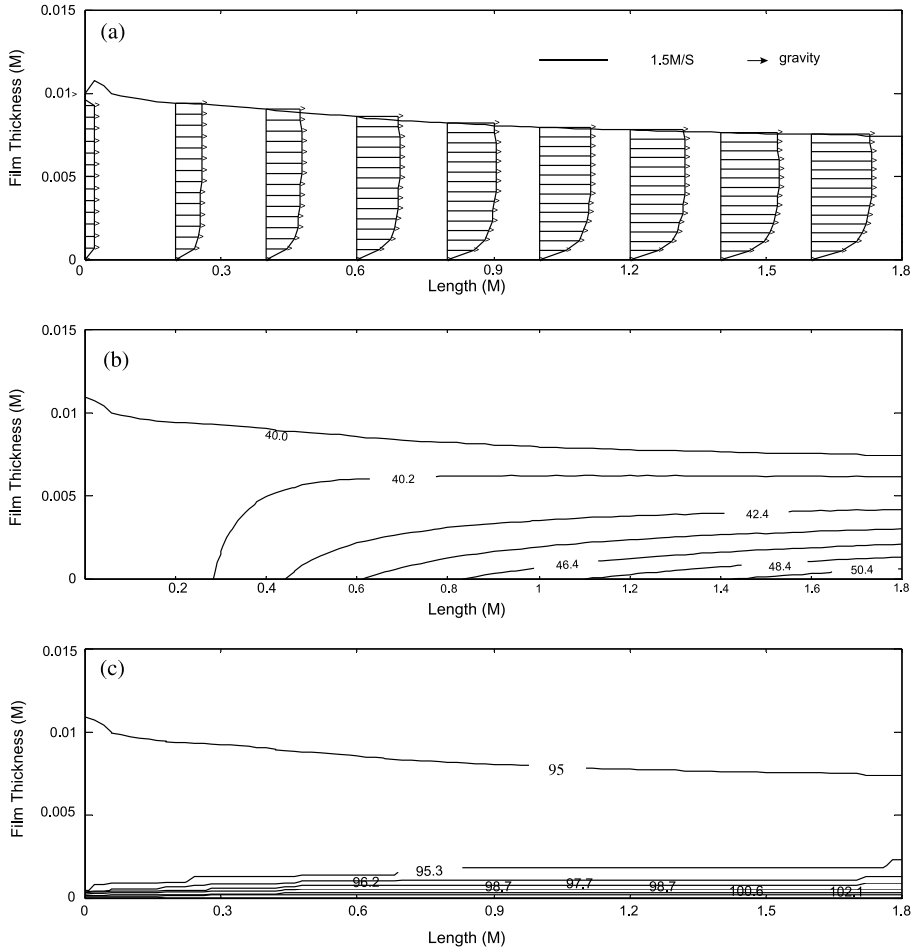

Fig. 4. Profiles of velocity (a), black liquid concentration (b), and temperature (c) in a 1.8-m-long falling film. The Reynolds and Prandtl number are 2650 and 19.6, respectively.

the fluid stream expands slowly because of the turbulent interaction of water vaporization, as would also occur in the case of a 10-m-long falling film.

In Fig. 4(c), a very steep temperature gradient is seen in the viscous sublayer near the heated surface. The peripheral temperature of falling film, however, has no variation, as is illustrated more significantly in Fig. 5(a). This lack of variation is due to the short contact time between the process fluid and the heat transfer surface. Another reason is that the Prandtl number of black liquor is quite high. All the heat supplied from the heated wall is absorbed within the viscous sublayer, which leads the temperature profile to become uniform beyond it. In the current case, the contact time is less than 2 s and the Prandtl number is 19.6; by comparison, the Prandtl number of water is 1.9 at the same condition. As the length of the falling film increases, the temperature of the falling film periphery would be affected to some degree, as illustrated in Fig. 4(c).

Consequently, the concentration of the black liquor solids occurs in a similar way. The vaporization of water species always occurs within the sublayer closest to the heated surface because of the rapid temperature variation there. The volume fraction of the liquid phase at the sublayer of the falling film is significantly reduced compared with its neighboring zone (Fig. 5(b)). The very thin zone is dominated by a vapor-enriched two-phase flow, and the black liquor solids concentration is enriched there as well. The highest solids concentration of black liquor is found near the heat transfer surface, and the other locations show a slow decay in the concentration value from the heat transfer surface to the falling film periphery, as seen in Fig. 4(b). This situation is due to the strong turbulence and diffusion caused by evaporation inside the falling film, as illustrated in Fig. 3(c) and (d). Maximum turbulent dissipation exists at the heat transfer surface, where the vaporization of water species happens. In addition, the high turbulent dissi-

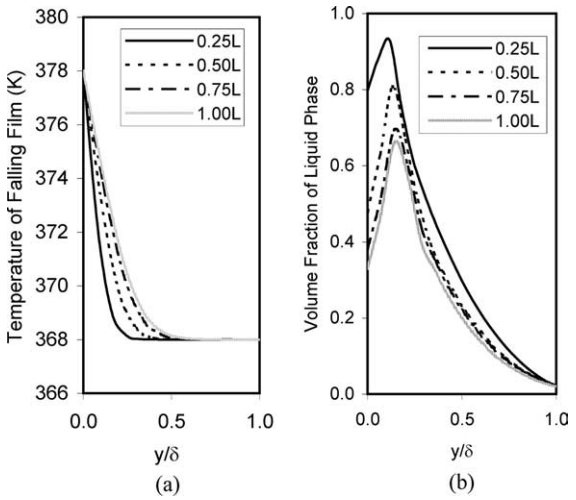

Fig. 5. Transverse profiles of film temperature and the volume fraction of liquid phase in a 1.8-m-long falling film; The Reynolds and Prandtl number are 2650 and 19.6, respectively.

pation benefits the transport of the black liquor solids concentration from the high to the low zone.

To further understand the flow dynamics characteristics of a falling film evaporator, it is necessary to investigate the performance of a pure liquid falling film, which has no evaporation process. In the study, one case is considered without heat and mass transfer between the gas and liquid phases. Fig. 6 shows the velocity profile of a pure liquid falling film. A pure liquid falling film is considered to be a fully developed flow at 1.2 m away from the entrance. Compared with Fig. 4(a), two significant differences are found. First, the film thickness of a pure liquid falling film decreases, as illustrated in Fig. 6. Its film thickness decreases 25% more than that of an evaporative falling film. The second difference is the flow characteristics of a falling film, caused by the evaporation process in the sublayer close to the heated surface. The evaporation process forces an evaporative falling film to expand in thickness and become unstable. The simulation result shows that a pure liquid falling film always keeps the single phase present. However, an evaporative falling film develops significantly into two-phase flow, although the falling film is still dominated by the single phase at the entrance.

4.2. Effect of solids concentration and thermal boundary

Black liquor enrichment is strongly sensitive to the black liquor solids concentration and thermal boundary condition. Fig. 7 plots the effect of black liquor solids concentration and thermal boundary condition on the enrichment of the solids concentration at the exit of a 1.8 m-long falling film.

The thermal properties of black liquor are strongly dependent on black liquor solids concentration. For 35%, 40% and 45% black liquor solids concentrations, their Prandtl numbers are 14.8, 19.8, and 33.1, respectively. Usually, a high Prandtl number results in low thermal diffusion. In Fig. 7(a), the black liquor solids concentration is illustrated as diminishing from the heated wall to the periphery of the falling film, and the major enrichment of black liquor occurs within the small zone. On the other hand, black liquor solids concentration also affects the movement of falling film. The Reynolds numbers of 35%, 40% and 45% black liquor solids concentration are 3552, 2649, and 1568, respectively. A higher Reynolds number is positive in forming a thinner faster-flowing film coating the vertical heated surface, which results in a higher heat transfer coefficient. This is beneficial to the enhancement of black liquor enrichment. The enrichment of black liquor with a high Reynolds number is more effective and efficient than that of a mixture with a low Reynolds number. For example, after the enrichment of black liquors at Reynolds numbers of 3552, 2649 and 1568 in a 1.8-m-long falling film, their bulk solids concentrations increase by 3.2%, 2.8%, and 2.1%, respectively.

Fig. 7(b) illustrates the effect of the surface-to-bulk temperature difference on black liquor enrichment. The effect of the surface-to-bulk temperature difference on black liquor enrichment is significant, especially near the surface of a heated wall. Adjusting this difference is an

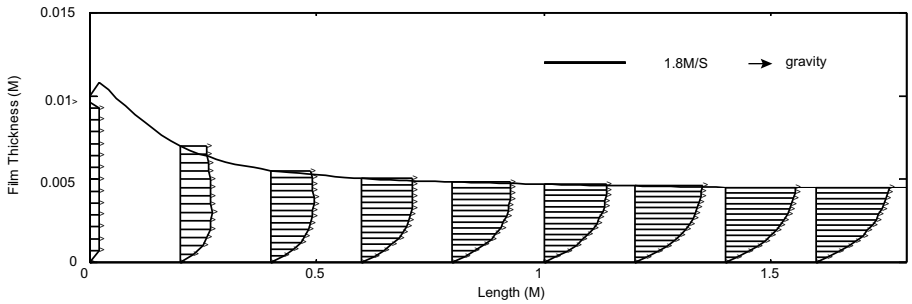

Fig. 6. Profile of velocity in a 1.8-m-long pure liquid falling film. The Reynolds and Prandtl number are 2650 and 19.6, respectively.

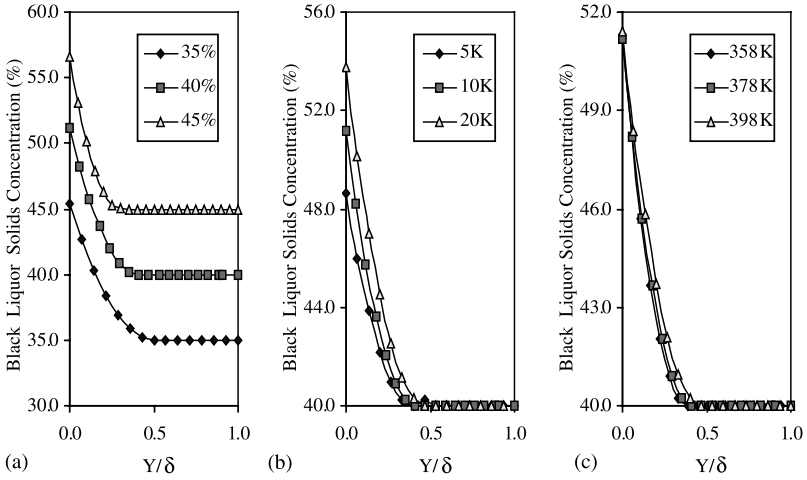

Fig. 7. Effect of soluble solids concentration and thermal boundary condition on black liquor enrichment at the exit of a 1.8-m-long falling film (a) is soluble solids concentration; (b) is surface-to-bulk temperature difference; (c) is wall temperature.

effective method of controlling black liquor solids enrichment. A difference of within 5–10 K is reasonable to enrich black liquor and minimize scale fouling if the bulk black liquor solids concentration is higher than 40%. Meanwhile, it could improve the productivity of the whole process without any scale fouling if adopting a higher surface-to-bulk temperature difference for a low-solids black liquor effect in a multi-effect system.

The temperature of the heated surface slightly affects the enrichment of black liquor. This is because black liquor is a heat-sensitive fluid. Varying heated surface temperatures would affect the soluble limitation and bulk liquid properties further, to modify the black liquor flow. Fig. 7(c) shows that a higher temperature on the heated surface has a positive effect on improving the concentration process for black liquor, which is meaningful to the enrichment of low-solids black liquor in a multi-effect system.

4.3. Fouling of black liquor in a 1.8-m falling film evaporator

Fouling control is a critical problem experienced in pulping and paper mills (Muller-Steinhagen and Branch, 1997). Precipitation and scale fouling occurs if the black liquor solids concentration is beyond the solubility limit. Therefore, an understanding of the crystallization and scaling mechanisms will aid in finding a solution to minimize the formation of these encrustations.

Recently, Föster et al. [31] and Muller-Steinhagen and Branch [30] presented the empirical models for predicting heat transfer fouling. These models were not suitable to predict scale fouling of black liquor because they did not consider the critical solids point for fouling of black liquor. A modified phenomenological model based on soluble solids concentration and Muller-Steinhagen's and Branchs' empirical model [30] is presented to generalize the mechanisms leading to fouling, as well as find the governing process parameters. The revised model considers the following assumptions: (1) the deposition process is controlled by a chemical reaction on the heat transfer surface; (2) there is a positive concentration driving force between the bulk and surface; and (3) the system is considered as a quiescent, diffusion-controlled system. Based on these factors, the precipitation of black liquor is described as:

$$\frac{\partial m}{\partial t} = K_r (C_b - C_s)^n. \tag{16}$$

The foregoing equation is a general order rate equation of a chemical reaction. For a quiescent, diffusion-controlled system, n would be equal to one. The surface rate constant K_r is assumed to follow the Arrhenius equation:

$$K_r = K \exp\left(-\frac{E_{act}}{RT_s}\right). \tag{17}$$

Based on the following equation, the deposition rate per unit area is related to the fouling resistance.

$$\frac{\partial m}{\partial t} = \rho_d \lambda_d \frac{\partial R_f}{\partial t}, \tag{18}$$

where ρ_d and λ_d are the deposit density and thermal conductivity, respectively. Thus, the fouling resistance could be written by

$$\frac{\partial R_f}{\partial t} = \frac{Ka}{\rho_d \lambda_d} \exp\left(-\frac{E_{act}}{RT_s}\right)(C_b - C_s), \tag{19}$$

where $E_{act} = \alpha E_0$, $C_b - C_s = \rho_{bl}(c_b - c_s)$, and $c_s = 0.8547–0.0147 \cdot Z - 0.0095 \cdot W$.

An analysis based on the experimental data [30] provided an estimate of the constants in the equations, such as $\frac{\rho_{bl} Ka}{\rho_d \lambda_d} = 0.072$ m^2 K/kW min, $E_0 = 3431$ kJ/kmol, and $\alpha = 0.95 + 10c_s/(\theta + 30)$.

Fig. 8 illustrates the validation results between the predicted and experimental data. The experimental data came from Smith and Hsieh's experimental test [1], which was conducted at a 383 K steam temperature, a 10-gpm circulation rate, and 0.75 Na_2CO_3/Na_2SO_4. Fig. 8 illustrates that the current model is reasonably accurate in predicting the fouling process in black liquor falling film.

Fig. 9(a) illustrates that the inlet bulk solids concentration of black liquor has a significant effect on the fouling rate in a black liquor falling film evaporator. When the inlet solids concentration is 45%, the fouling resistance is five times higher than when it is 40%. No fouling appears if the inlet black liquor concentration is 35%. The maximum soluble solids concentrations of 35%, 40%, and 45% black liquor at the heated wall are 45.4%, 51.2%, and 56.6%, respectively. The latter two are beyond the critical solids point, which could result in severe scale fouling. Therefore, when the black liquor solids concentration is high, a strategy is needed to control fouling.

As a heat-sensitive fluid, the surface-to-bulk temperature difference and thermal boundary condition are important factors in controlling black liquor fouling rate, as seen in Fig. 9(b) and (c). The foregoing analysis pointed out that increasing the surface-to-bulk temperature difference has a positive effect on the enrichment of black liquor. A large surface-to-bulk temperature difference, however, is shown to accelerate the scaling rate in Fig. 9(b). The inclination becomes more severe with an increase in the heat transfer temperature difference. In particular, a large surface-to-bulk temperature differential has a strongly negative effect on controlling scale fouling for a black liquor with a high solids concentration. The ideal surface-to-bulk temperature difference is around 5–10 K. It is also seen in Fig. 9(c) that wall temperature has a slight effect on scale fouling. A low wall temperature is positive for soluble scaling control. The soluble limitation of black liquor is in opposition to temperature. The scale fouling of black liquor is strongly related to enrichment; thus optimization of the thermal boundary is necessary to reduce the fouling of black liquor in a falling film evaporator. The current analysis suggests that a lower surface-to-bulk temperature difference and lower surface temperature are reasonable ways to improve both concentration enrichment and control of soluble scaling for a high-solids-concentration black liquor.

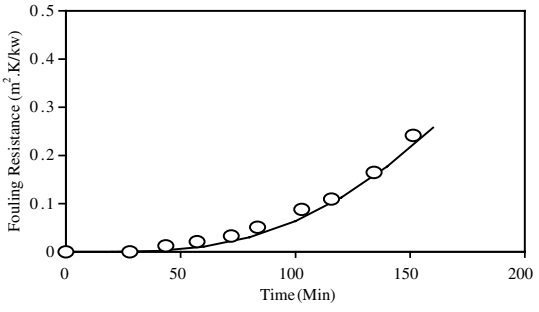

Fig. 8. Comparison between the predicted and experimental data from Smith and Hsieh [1].

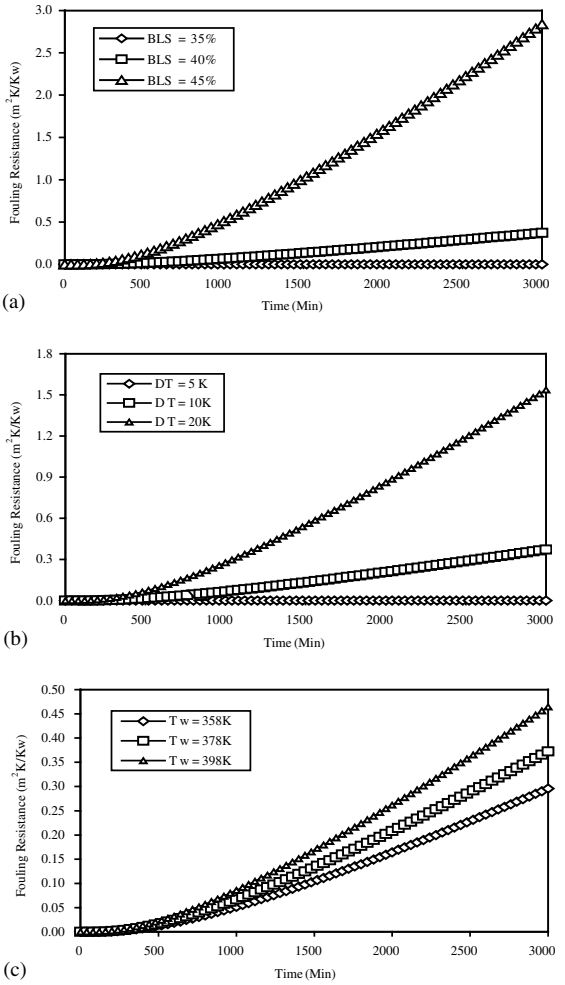

Fig. 9. Effect of soluble solids concentration and thermal boundary condition on fouling resistance as a function of time (a) is soluble solids concentration; (b) is surface-to-bulk temperature difference; (c) is wall temperature.

4.4. An industrial case study

Unlike the equipment in the testing laboratory, an industrial-scale falling film evaporator is usually as tall as 6–10 m [1]. A study based on a 10-m-long falling film evaporator was carried out to simulate performance at the industrial scale. The study conditions were a black liquor flow of 0.2 m/s, a wall temperature of 378 K, an initial black liquor solids concentration of 40%, and a heat transfer temperature difference of 10 K.

Fig. 10 shows the profiles of velocity, temperature, and black solids concentration within a 10-m-long falling film. In Fig. 10(a), the entire phenomenon of the vena contracta is more pronounced than in Fig. 3(a). Significantly, the process fluid expands slowly through turbulent interaction with a gas stream after the vena contracta. Although the major temperature gradient still occurred within a thin, highly viscous sublayer, the peripheral temperature gradient of the falling film did not remain flat as it did previously, as plotted in Fig. 10(c). The numerical data illustrate that this is the consequence of vapor migration within the falling film. Fig. 10(b) shows the profile of the soluble solids concentration.

Fig. 11(a) illustrates the effect of falling film length on black liquor enrichment. From Fig. 11(a), the bulk black liquor solids concentration is enriched from 40% to 48%. Therefore, a 10-m-long falling film evaporator is suitable to serve as a high concentration effect in a multi-effect system. The phenomenon of this enrichment is closely related to heat transfer and turbulent process. A higher heat transfer coefficient between the liquid film and the

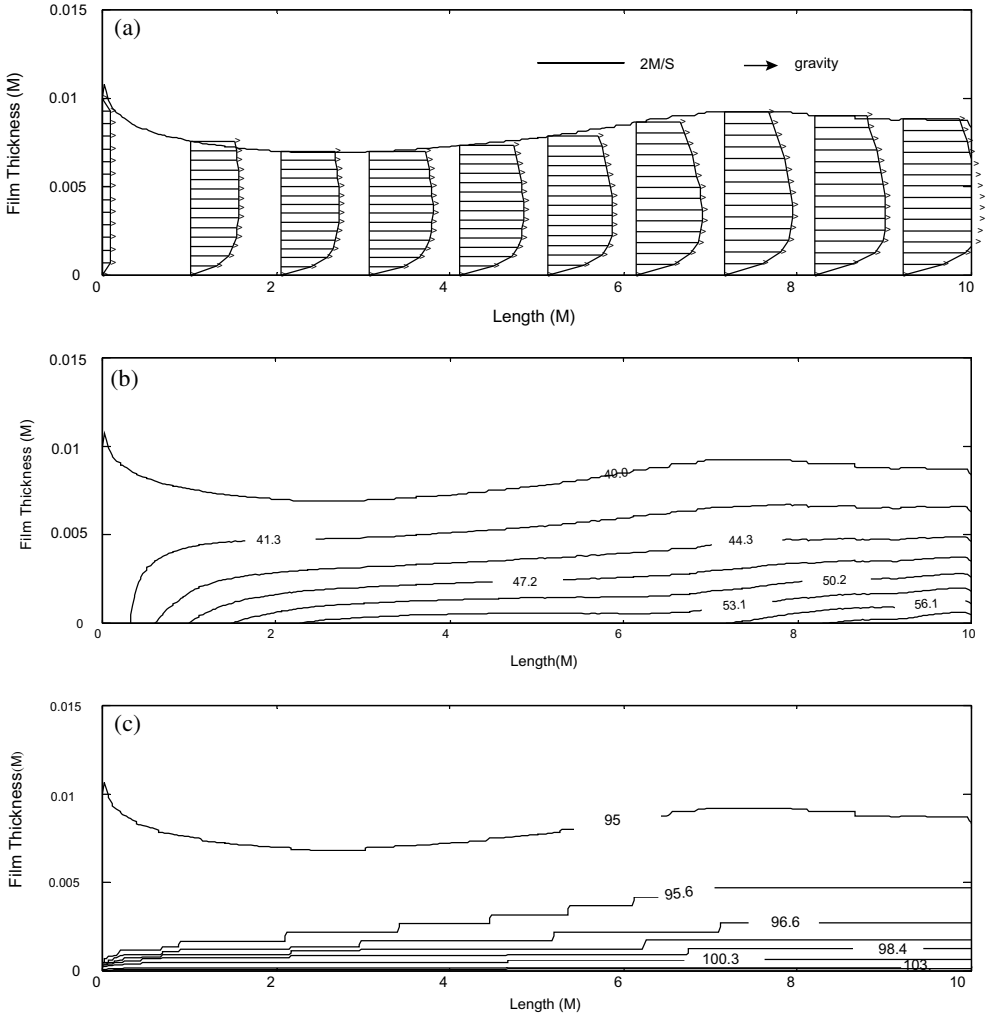

Fig. 10. Profile of velocity (a), black liquor concentration (b), and temperature (c) in a 10-m-long falling film.

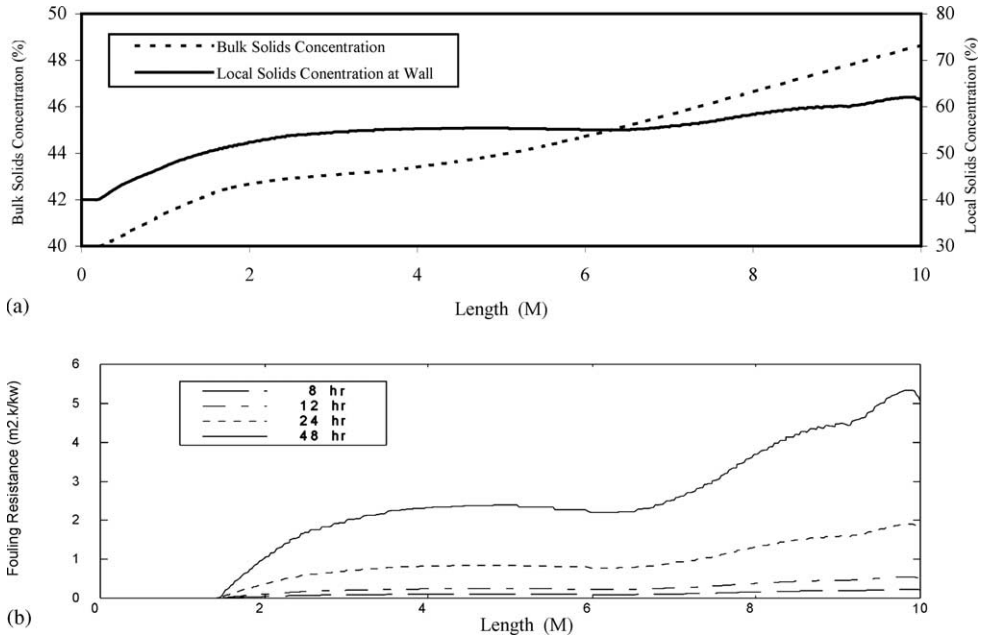

Fig. 11. Effect of the length of falling film on bulk solids concentration enrichment, local solid concentration at wall, fouling resistance.

heated wall leads to rapid black liquor enrichment after a short entrance region; then the bulk enrichment becomes flat because plenty of vaporized water dominates the zone close to the heat transfer surface; finally the length of the falling film is over 6 m, the bulk enrichment is enhanced due to strong turbulent diffusion. In the 10-m-long falling film, however, there is a region where the black liquor solids concentration is beyond the critical solids point. From Fig. 11(a), the maximum soluble solids concentration of local black liquor along the wall is nearly 60%. This concentration will result in precipitation and fouling on the heat transfer surface.

Fig. 11(b) shows the fouling resistance profile of the 10-m-long falling film as a function of falling film location and time. Over time, the fouling resistance becomes more significant, especially after 24 h. Soluble scale fouling is closely related to the soluble black liquor solids concentration. Consequently, the bottom region of the falling film suffers more severe fouling resistance than others. Therefore, a periodic wash is still important to maintain continuous performance in a modern pulp mill. Fig. 11(a) also illustrates fouling resistance as a function of time and of the length of the falling film. It has been found that there is no significant fouling of a 1.8-m-long falling film on the heat transfer surface. However, fouling becomes worse as the length of the falling film increases at a certain running time. For a 6-m-long falling film, fouling becomes worse after 36 h, while fouling for a 10-m-long film is relatively worse in 24 h.

5. Conclusion and recommendation

In this paper, a computational fluid dynamics model based on a turbulent two-phase flow with multi-components is presented to investigate the transport processes of black liquor falling film into a rising vapor stream. The results illustrate that most of the heat and mass transfer of black liquor film occurs at a very thin viscous sublayer close to the heat transfer surface. Vaporized water dominates the zone. The concentration of black liquor is caused by water vaporization and highly related to the length of the falling film. The further prediction illustrates that evaporation annihilates part of the downward momentum of a falling film, leading the velocity of an evaporative falling film to be less than that of a pure liquid falling film.

The influence of both soluble solids concentration and thermal boundary conditions on the enrichment in a black liquor falling film evaporator is investigated in detail. The results illustrate that a higher surface-to-bulk temperature difference is positive to low-solids black liquor enrichment.

A crystallization fouling based on a non-equilibrium chemical reaction at a heated surface is presented to analyze the scale fouling of black liquor. The current fouling model could be used to estimate an optimal cleaning cycle for black liquor evaporators. Soluble scale fouling from black liquor is very sensitive to the liquor solids concentration and the thermal boundary condition. For a higher-solids black liquor, a high Reynolds

number, a low surface-to-bulk temperature difference, and a low surface temperature could be effective methods of improving both the liquor enrichment and soluble scale control.

In a 10-m-long falling film, the bulk black liquor solids concentration can be enriched from 40% to 48.5%. The local soluble solids concentration close to the wall around the bottom could be beyond the critical solids point, where soluble scale fouling may form on the vertical heated surface. Therefore, a 10-m-long falling film is a reasonable way to achieve a high-concentration effect in a multiple-effect evaporator to minimize the extent of fouling.

Additional thermophysical properties data for black liquor will be needed to further investigate the design of black liquor falling film evaporators to optimize their performance.

Acknowledgements

This work was performed at the Oak Ridge National Laboratory, which is managed by UT-Battelle, LLC, under contract DE-FG36-99GO10387 for the US Department of Energy. The work was sponsored by the US Department of Energy as a collaborative effort with the Institute for Paper Science and Technology and Georgia Institute of Technology on controlling soluble scale fouling in black liquor evaporators.

During the course of this study, assistance and valuable information were given by Drs. W.J. Frederick and. G.W. Schmidl of IPST and Dr. J.S. Hsieh of Georgia Tech. The authors are grateful to Dr. V.C. Mei and many colleagues at Oak Ridge National Laboratory who have provided positive suggestions and ideas helpful to our efforts.

References

[1] J.B. Smith, J.S. Hsieh, Improvements on falling film black liquor evaporator: final technical report, United States Department of Energy Report, Sub Contract #85XRS68IC, September 1999.
[2] R.H. Hedrick, J.S. Kent, Crystallizing sodium salts from black liquor, TAPPI J. 75 (12) (1992) 107–111.
[3] G.W. Schmidl, W.J. Frederick, Controlling soluble scale deposition in black liquor evaporators and high solids concentrators, Internal Report, IPST, 1999.
[4] T.M. Grace, A survey of evaporator scaling in the alkaline pulp industry, Institute of Paper Chemistry Project 3234, Report One, 1975.
[5] A. Süren, Scaling of black liquor in a falling film evaporator, Master Thesis, Georgia Institute of Technology, Atlanta, GA, 1995.
[6] M.A. Rosier, Model to predict the precipitation of burkeite in the multiple-effect evaporator and techniques for controlling scaling, TAPPI J. 80 (4) (1997) 203–209.
[7] B. Shi, R.W. Rousseau, Crystal properties and nucleation kinetics from aqueous solutions of Na_2CO_3 and Na_2SO_4, Indust. Eng. Chem. Res. 40 (2001) 1541–1547.
[8] A.A. Zaman, A.L. Fricke, Newtonian viscosity of high solids kraft black liquor: effect of temperature and solids concentration, Indust. Eng. Chem. Res. 33 (1994) 428–435.
[9] A.A. Alhusseini, K. Tuzla, J.C. Chen, Falling film evaporation of single component liquids, Int. J. Heat Mass Transfer 41 (12) (1998) 1623–1632.
[10] W. Nusselt, Die oberflächenkondensation des wasserdampfes, Z. Ver. Deut. Ing. 60 (1916) 541–546, 569– 575.
[11] G. Karimi, M. Kawaji, An experimental study of freely falling film in a vertical tube, Chem. Eng. Sci. 53 (20) (1998) 3501–3512.
[12] A. Stücheli, M.N. Özisk, Hydrodynamic entrance lengths of laminar falling film, Chem. Eng. Sci. 31 (1976) 369–372.
[13] P. Adomeit, U. Renz, Hydrodynamics of three-dimensional waves in laminar falling films, Int. J. Multiphase Flow 26 (2000) 1183–1208.
[14] R.A. Seban, Transport to falling film, Proceedings of the Sixth International Heat Transfer Conference, vol. 6, Toronto, Canada, 1978, pp. 417–428.
[15] J.D. Killion, S. Garimella, A critical review of model of couple heat and mass transfer in falling-film absorption, Int. J. Refrig. 24 (2001) 755–797.
[16] R.A. Seban, A. Faghri, Evaporation and heat with turbulent falling liquid films, J. Heat Transfer 98 (2) (1976) 315–318.
[17] K.R. Chun, R.A. Seban, Heat transfer to evaporating liquid film, J. Heat Transfer 93 (3) (1971) 391–396.
[18] M.L. Yüksel, E.U. Schlünder, Heat and mass transfer in non-isothermal absorption of gases in falling liquid Films, part II: theoretical description and numerical Calculation of turbulent falling film heat and mass transfer, Chem. Eng. Process. 22 (1987) 202–213.
[19] T.S. Chen, C.F. Yuh, Combined heat and mass transfer in natural convection on inclined surfaces, Num. Heat Transfer 2 (2) (1979) 233–250.
[20] J. Schroppel, F. Thiele, On the calculation of momentum, heat and mass transfer in laminar and turbulent boundary layer flows along a vaporizing liquid film, Num. Heat Transfer 6 (1983) 475–496.
[21] T.R. Shembharkar, B.R. Pai, Prediction of film cooling with a liquid coolant, Int. J. Heat Mass Transfer 29 (6) (1986) 899–908.
[22] W.W. Baumann, F. Thiele, Heat and mass transfer in two-component film evaporation in a vertical tube, The 8th International Heat Transfer Conference, vol. 4, 1986, pp. 1843–1848.
[23] W.M. Yan, Evaporative cooling of liquid film in turbulent mixed convection channel flow, Int. J. Heat Mass Transfer 41 (1998) 3719–3729.
[24] Y.L. Tsay, T.F. Lin, Evaporation of a heated falling liquid film into a laminar gas stream, Exp. Therm. Fluid Sci. 11 (1995) 61–71.
[25] R. Ramamurthy, Adriaan R.P. van Heiningen, K.J. George, Viscosity and thermal conductivity of black liquor, TAPPI J. 76 (11) (1993) 175–179.
[26] F.P. Incropera, D.P. DeWitt, Introduction to Heat Transfer, third ed., John Wiley & Sons, 1996, pp. 764–765.

[27] S.V. Patankar, D.B. Spalding, A calculation procedure for heat, mass and momentum transfer in three-dimensional parabolic flows, Int. J. Heat Mass Transfer 15 (1972) 1787–1806.
[28] S. Portalski, Velocities in film flow of liquid on vertical plates, Chem. Eng. Sci. 19 (1964) 572–582.
[29] J.O. Wilkes, R.M. Nedderman, The measurement of velocities in thin films of liquid, Chem. Eng. Sci. 17 (1962) 177–186.
[30] H. Muller-Steinhagen, C.A. Branch, Heat transfer and heat transfer fouling in kraft black liquor evaporators, Exp. Therm. Fluid Sci. 14 (1997) 425–437.
[31] M. Föster, W. Augustion, M. Bohnet, Influence of the adhesion force crystal exchanger surface on fouling mitigation, Chem. Eng. Process. 38 (1999) 449–461.
[32] W.J. Frederick, G.W. Schmidl, et al., Control of Soluble Scale Fouling in High-Solids Black Liquor Concentrators, Final Technical Report, IPST, 2003.